

Residual rubber shielded multi walled carbon nanotube electrodes for neural interfacing in active medical implants



K. Tegtmeier*, Pooyan Aliuos, T. Lenarz, T. Doll

Cluster of Excellenz "Hearing4 All" at Hannover Medical School, Carl-Neuberg-Str. 1, 30625 Hannover, Germany

ARTICLE INFO

Article history:

Received 29 March 2016

Received in revised form

4 April 2016

Accepted 4 April 2016

Available online 13 April 2016

Keywords:

Carbon nanotubes

PDMS

Active neural implant

Biocompatibility

ABSTRACT

Advanced neuroprostheses need high density, mechanically flexible contacts with superior electro-physiological performance. Carbon nanotubes have shown interweaving with neurites are well suited but are opposed by ongoing nanoparticle biocompatibility discussions. We present a route circumventing those issues by immersing multiwalled carbon nanotubes (MWCNT) in silicone rubber and re-etch the surface yielding a MWCNT-lawn electrically contacted towards the percolative bulk. The use of tetra-n-butylammonium fluoride (TBAF) and sodium hydroxide solution (NaOH) leads to desired freestanding CNT strands still covered by residual rubber of approximately 13 nm thickness. The biocompatibility of such interfaces has been proven by WST-1-Assays for cell metabolism of 3T3NIH fibroblasts and SH-SY5Y neuroblastoma cells in terms of growth and morphology. Neural cell adhesion is proven with biomolecular markers. The electrical performance reaches percolation conductivities of up to 1.6×10^2 S/m. The lowest impedance was $1.3 \times 10^2 \Omega \text{cm}^2$ at 1 kHz, which is similar to gold reference electrodes whilst their capacitive roll off is lowered in electrophysiological arrangements. When compared to pure MWCNTs the performance is decreased due to the insulating residual rubber encasement. However, this is seen to be a reasonable loss in the light of the increased biosafety of rubber shielded MWCNT neural interfaces.

© 2016 The Authors. Published by Elsevier B.V. This is an open access article under the CC BY license (<http://creativecommons.org/licenses/by/4.0/>).

1. Introduction

The advancement of medical devices faces strong issues on quality and risk assessment when new materials get introduced. This rapidly triggers cascades of biocompatibility testing, especially when "nano"-formulations are intended to be used in active stimulating neuroprostheses. All cochlea-, retina- or peripheral nerve implants use electrode arrays as contacts for selective electrical stimulation of nerve fibres or neurons to restore sensory or motor functions. Whilst platinum or platinum-iridium contacts are mature in clinical use, other materials are investigated for superior charge transfer characteristics and improved low frequency impedances.

One issue regarding the functional improvement of neuroprostheses is the increase in the number of electrode contacts to achieve higher selectivity when electrically stimulated. Though, there are limitations in minimizing the electrode contact's size (area), since a decreased electrode surface area may lead to high

current densities, conflicting with the electrochemical safety requirements [1]. Electrochemical changes not only generate abnormalities in the structure and function of cells, they also damage the electrode contacts [2] and therefore need to be minimized. The increase of the number of connecting wires towards the implants electronics is associated with an increased number of electrode contacts, leading to an elevation of rigidity in the electrode array. Implantation of a too rigid electrode array very likely ends with damage of the soft neural tissue either during the insertion of the electrode array or due to low mechanical compliance towards tissue movements. In general, for new electrode designs based on novel materials possessing good conductive and elastic properties, a parallel investigation of biocompatibility is indispensable. Amongst present candidates there are micro- and nanostructured platinum-iridium with increased effective surface [2], iridium-oxide modifications with superior electrophysiological maximum charge limits [3], conducting polymers like polypyrrole and PEDOT [4] and carbon electrodes based on graphite/graphene as well as carbon nanotubes in various variants and oxidation states [5–8]. The advantage of the carbon system arises primarily from its electrochemical window that fits better to cell tissues than the noble metals with high work function values [9]. Whereas from all

* Corresponding author.

E-mail address: tegtmeier.katharina@mh-hannover.de (K. Tegtmeier).

allotypes carbon nanotube layers provide a morphology that seems to be perfectly adopted towards interweaving with neural axon and dendrite structures, they have raised a still ongoing discussion in biocompatibility. This paper explores a route to circumvent the latter issues whilst preserving good interface properties. Carbon nanotubes (CNTs) are cylindrically rolled graphene sheets with a high aspect ratio, resulting from small diameters in the low nanometre range, but lengths in the micron scale. Single-walled CNTs (SWCNTs) consist of one rolled-up graphene sheet, while coaxially stacked multi-walled CNTs (MWCNTs) consist of many concentrically arranged tubes [10,11]. They have metallic or semiconducting electrical properties, depending on the chirality of the graphene roll. The conductivity of MWCNT is not improved by the inner shells, as their coupling to the outer layer is weak [10]. Nevertheless, MWCNTs show larger electrochemically accessible surface areas than the SWCNTs making them a more promising choice for interfacing neurons. Besides their wide use as biosensors e.g. for DNA [12] or as bioseparators and –catalysts [13], CNTs have already been used for neural recording and stimulation both *in vitro* and *in vivo*. For example, Gaillard et al. have successfully used MWCNT as neural cell substrates and recorded signals from primary splenocytes and neurons [14]. Another study revealed enhanced adhesion of neurons, when they were cultivated on MWCNT substrates. Tight contacts between neural cell membranes and MWCNTs were observed, suggesting electrical shortcuts between distal and proximal cell parts [15].

When compared to conventional electrode materials the use of CNTs for interfacing neurons promises an improvement of the general electrical characteristics in both stimulation and recording such as signal to noise ratio (SNR) and safe charge injection density, since a more effective surface area is delivered [10,16,17]. Nevertheless, there are also studies indicating harmful effects of CNTs especially in suspended form. For example, Hanna et al. showed highly toxic effects of suspended MWCNTs (conc. 40 $\mu\text{g}/\text{ml}$) and induction of DNA damage in A549 lung endothelial cells of mice [18]. Also *in vivo* studies revealed e.g. asbestos-like pathogenicity or the initiation of mesothelioma in mice, when long (length > 5 μm) non-functionalized MWCNT were administered in the abdominal cavity. However, these cytotoxic effects were hypothesized to be caused by the size and shape similarity between CNTs and asbestos [19,20]. As described above, the biocompatibility of CNTs seems to depend extensively on their size. Also their possible transport inside the body needs consideration, as lung, liver and spleen seem to bear the largest inflammatory potential against these nanoparticles [21]. In order to avoid such transport from neural structures to other organs we developed the concept of anchoring CNTs in silicone rubber. This idea relates to the use of CNTs in rubber in electroencephalographic recording electrodes instead of classic wet electrodes. But, whilst these electrodes may come with high specific contact impedance like 100 $\text{k}\Omega\text{ cm}$ [2], stimulation seeks always for values as low as 100 $\Omega\text{ cm}^2$.

In order to achieve this and regain a neurite mimicking surface morphology we started to partially recess the topmost silicone rubber in order to obtain, in simple view, some sort of a freestanding CNT-lawn. As the routes of silicone rubber etch involve possibly harmful substances like NaOH and TBAF it was necessary to investigate the biocompatibility of such treated surfaces and then classify the resulting impedances in comparison to the state of the art. First test results as reported here, need to take into consideration that on the nanoscale, silicone rubber etch routinely leaves a residual rubber film: Beigbeder et al. [22] showed with simulations of PDMS-CNT compounds that CH_3 - π interactions are a driving force towards a wrapping of the polymer chains around CNT which lead towards exceptional etching resistance of the first polymer layers. The latter fact may, on the one hand help with

biocompatibility but, on the other hand may be a detriment to the electrical contacting properties of such interfaces.

2. Material and methods

2.1. Sample preparation

The compound under investigation consists of MWCNTs immersed in Sylgard 184, a two component room temperature vulcanized polydimethylsiloxane (PDMS, Dow Corning, USA). Two types of CNTs are used, for analysing differences in conductivity and processing. C150P (Bayer Materials Science, Germany), also called Baytubes, have a purity of >95% and an outer diameter of 13–16 nm according to the data sheet and NC7000 (Nanocyl, Belgium) have a purity of 90% and a mean outer diameter of 9.5 nm according to the data sheet. Both are produced by chemical vapour deposition and contain potentially cytotoxic catalyst residues which, for enhanced biomedical safety, need to be eluted in later stages of the development. For sample preparation, CNTs were manually immersed in silicone rubber inside a glove box, followed by a mixing procedure using a mortar. No further mixing techniques were applied to disentangle or align CNTs, due to failure of available techniques. Nanocompounding [24] was not possible with incorporated NC7000 and sonication did not lead to agreeable results for both compounds. To evaluate the percolation threshold different amounts of CNTs were mixed into the compound, using weight percentage to define the amount of CNTs. The compound was mixed with the PDMS curing agent in a 1:10 ratio. CNT-silicone rubber samples were produced on glass substrates (Süsse Objektträger, Süsse Labortechnik, Germany) in lost castings, which can be used to vary the samples thickness in 54 μm steps. After spreading the material in the cast using a fountain blade, it was cured at 100 $^\circ\text{C}$ for 45 min. Different sample sizes and thicknesses were used for the material analysis, which are mentioned in the relating chapters.

2.2. Wet-etching of CNT-silicone rubber surface

Complete immersion of the CNTs, as done in this compound, not only prevents to CNTs from leaching from the material, but also leads to insulation towards the cells which are to be stimulated or recorded. Since low impedance is necessary in both cases, the surface PDMS needs to be recessed towards almost freestanding CNTs bearing remainder PDMS layers allowing for electron tunnelling. The samples used for these etching procedures were 162 μm thick and cut into 5 mm \times 5 mm pieces for easy handling. Two different etchants, tetra-*n*-butylammonium fluoride solution (75% (w/w) in H_2O , Sigma Aldrich; TBAF) and sodium hydroxide (5% (w/w) in purified water, Sigma Aldrich, NaOH), were tested. TBAF is used for its fluoride ions, which can break down the strong Si–O-bonds in the silicone rubber [23]. The samples were covered with the etchant in a soda lime petri dish for different time periods. Following that, they were repeatedly rinsed with purified water, to remove any traces of the chemicals on the samples. Whilst TBAF etching was done at room temperature, the NaOH solution was applied at an elevated temperature of 50 $^\circ\text{C}$. The etching recipes refer to previous experience (Tegtmeier et al. [24]) with short etching times of 5 min. In this work, the etching periods were increased to 15 min, 30 min, 45 min, 60 min and 75 min.

2.3. CNT-silicone rubber analysis

The material investigation included measurements of the bulk conductivity as well as surface topography analysis and impedance measurements after etching.

Table 1
Amount of CNTs used in samples for bulk conductivity measurements in % (w/w).

C150P	NC7000
0.75 ^a	0.75
2.5 ^a	3.8
5	4.5
7.5	7.5
10	9.6
12.5	–

^a These were not used for the alignment.

The surface topography after etching was investigated using scanning electron microscopy (SEM). A FE-ESEM Quanta 400 F (FEI, USA) with a field emission cathode was used at an acceleration voltage of 20 kV in high vacuum. As the CNT-PDMS compounds are conductive, the samples did not need to be sputtered with gold. Therefore it was possible to directly inspect the thickness of the unveiled nanostructures and gather information on the amount of residual silicone rubber on the CNTs. The diameters were measured using the software available for this SEM.

Conductivity measurements of the bulk were performed using a 4-point measurement setup. The setup consists of a glass substrate, four copper contacts inside a mould and the CNT-silicone rubber, which is spread inside the mould, onto the contacts. Samples were cured and the resistance measured, using the 4-point-measurement principle. The same setup was used, to align CNTs in silicone rubber in a direct current (dc) electrical field. Each alignment started at 30 V while the changes in current were observed. When the changes in current stagnated, the voltage was increased by 10 V. The duration of each step depended on the sample and the amount of CNTs. The exact compositions, regarding the amount of both types of CNTs in the samples are displayed in Table 1. The material became increasingly brittle and difficult to process, the higher the amount of CNTs was, which sets the limit to the amounts used. Since it was discovered after the measurements on cured CNT-silicone rubber that low amounts of Baytubes lead to very high impedances the two lowest weight percentages of this material were not used for the alignment measurements.

A compound with only 0.15% (w/w) of NC7000 and no curing agent was used to align the CNTs in a DC-field to evaluate the polarization of the CNTs in the silicone rubber compound. Images were taken using an optical microscope (Stemi2000, Carl Zeiss microscopy). To investigate the etching effect on the surface impedance, electrochemical impedance measurements were

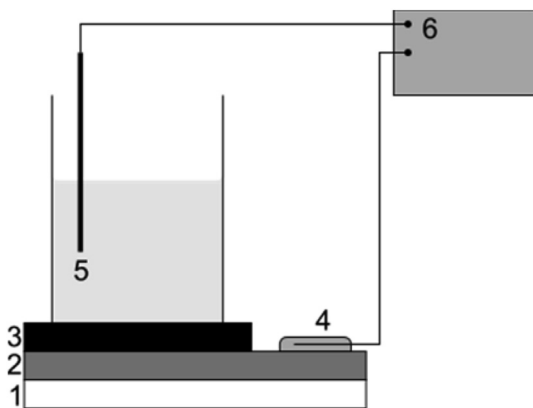


Fig. 1. Schematic of impedance measurement setup displaying 1) glass substrate, 2) copper foil, 3) CNT-silicone rubber, 4) conducting silver glue, 5) glass tube with NaCl solution and counter electrode and 6) impedance analyser.

performed. The impedance is measured using an electrochemical workstation IM6 (Zahner-Elektrik GmbH). The measurement setup (see Fig. 1) consists of a glass substrate and a self-adhesive copper foil glued to it on which the CNT-silicone rubber is applied in uncured condition and afterwards cured and etched as described above. A glass tube, filled with isotonic NaCl, is pressed onto the compound. The CNT-pad is contacted via conductive silver glue to the copper. The counter electrode (Ag/AgCl) is directly inserted into the NaCl. Samples measured were 7.5% (w/w) CNT-silicone rubber compounds. Both kinds of CNTs are used to investigate the impedance after etching with TBAF and NaOH for 15 min, 30 min, 45 min and 60 min. For comparison a glass substrate sputtered with 150 nm gold was also measured.

2.4. Biocompatibility test used on CNT-silicone rubber

To evaluate the biocompatibility of the CNT-silicone rubber, cell growth and morphology on the samples were investigated using lentivirally GFP-labelled murine NIH3T3 fibroblasts. To study neural cell growth and morphology, as well as cell adhesion, a human neuroblastoma cell line, SH-SY5Y, was used. Furthermore cell metabolism was investigated using a WST-1-Assay with native murine NIH3T3 fibroblasts.

All tests using fibroblast cells were done on both materials, while for the tests with SH-SY5Y only the Baytube material was used. The exact samples were a 7.5% (w/w) Baytube compound etched with TBAF for 45 min and 60 min and a 4.5% (w/w) NC7000 compound, etched with TBAF for 45 min and 60 min as well as with NaOH for 45 min and 60 min. All different cell types were cultured in Dulbecco's modified Eagle's medium (DMEM, Biochrom AG, Germany), supplemented with 10% (v/v) fetal calf serum (FCS, Biochrom AG) and 1% (v/v) penicillin (10,000 IE)/streptomycin (10,000 I g/mL; pen/strep, Biochrom AG). Cells were trypsinized and passaged every third day following the standard protocol.

For cell growth and morphology investigations with lentivirally GFP-labelled murine NIH3T3 fibroblasts, samples were placed into 24-well plates and fixed with polytetrafluoroethylene (PTFE)-rings to prevent them from floating. To allow easy placement in the wells and removal from the wells, the samples were fabricated with 810 μm thickness and cut into round samples with a diameter of 15 mm. 12,000 cells/ml were given to each well were they were grown until a monolayer was observed in the control well. Cells were fixed with paraformaldehyde (PFA, 4% (v/v) in phosphate buffered saline (PBS) 37 °C) and afterwards rinsed with PBS. PBS is an isotonic solution with a pH of 7.4 and consists of 137 mM sodium chloride, 2.7 mM potassium chloride and 12 mM phosphates. Cells were investigated using an Olympus BX51 fluorescence microscope (Olympus Europa GmbH, Hamburg, Germany).

To evaluate the cell growth, an ImageJ [25] Plugin was written to convert the images into 8-bit gray scale pictures and then counted the number of white pixels as cell body and black pixels as the background. By dividing the two parameters the percentage of cell growth on each sample surface was calculated.

Since the aim of fabricating electrode materials based on CNTs was their use as stimulating electrodes for application in neuroprostheses, their interaction with a neuron-like neuroblastoma cell line was evaluated to characterize any effects of CNT-silicone rubber on neural cell growth, adhesion and morphology by means of fluorescence microscopy. To study neural cell adhesion and growth, SH-SY5Y-cells with a concentration of 20,000 cells/ml were given to each well and the cells were allowed to grow for 24 h under cell culture conditions. The next day, the medium was replaced with medium containing retinoic acid (RA, Sigma Aldrich, Germany) (end conc. 20 μM) following the same protocol as used by Cheung et al. for initiating a neural differentiation of the SH-SY5Y cells [26].

This also leads to a halt in cell proliferation which leaves the cells with enough space in the well to differentiate and build a network. The culture medium was renewed every third day and the cells were fixed after 7 days of incubation.

To investigate the metabolism activity of native murine NIH3T3 fibroblasts, a water soluble tetrazolium dye (WST-1; Roche GmbH, Germany) was used. 10,000 fibroblasts were pipetted into each well of a 96-well plate and incubated until they reached about 80% confluency. The medium was then replaced by 100 μ l of DMEM without phenol red (Biochrom AG) and the samples were added to the wells and further incubated for 24 h. To some wells, instead of the samples, 100% Dimethyl sulfoxide (DMSO) was added as positive control to destroy the cells. Then 10 μ l of WST-1 solution (Roche, Mannheim, Germany) was added to each well and incubated for 3 h. Finally, well plates were shaken for 1 min and the optical density was measured via a microplate photometer (Multiskan Ascent, Thermo Scientific, USA) using a 450 nm filter. Cell viability is calculated using Equation (1) with cell viability in percent (*Cell viab %*), mean optical density of a certain sample (OD_{450s}) and the mean optical density of the control wells (OD_{450c}).

$$\text{Cell viab. \%} = 100 \times OD_{450s}/OD_{450c} \quad (1)$$

Since it is not guaranteed, that the mean optical density of the control wells is higher than that of the sample wells, it is possible to get cell viability values of >100%. In these cases, the cells thrived better on the samples, than on the control surface.

For neural cell adhesion studies SH-SY5Y cells were used on the Baytube compound to detect any changes in the adhesion and morphology of cells caused by the CNT-silicone rubber surfaces. Therefore neural cell adhesion molecules (NCAM) and neurofilaments (NF) were immunostained. Mouse monoclonal anti-neurofilament antibodies (mouse anti-200 kDa + 160 kDa neurofilament, cat. # ab24571, abcam, USA) and rabbit polyclonal anti-NCAM antibodies (rabbit anti-NCAM, cat. # ab95153) were diluted in PBS in a mixing ration of 1:200 and used as primary antibodies to stain NCAM-mediated adhesion as well as neurofilaments. STAR 440 SX goat anti-rabbit IgG and STAR 488 goat anti-mouse IgG (Abberior, Göttingen, Germany) were diluted in PBS (1:500) and used as secondary antibodies. Cells were cultivated on glass cover slips as control surfaces, on pure silicone surfaces and on the CNT-silicone rubber surface varieties as described before. After the cells were fixed, they were permeabilized using a 0.25% (v/v) Triton-X (Sigma Aldrich, Germany) solution (diluted in PBS) for 10 min. Samples were rinsed three times for 3 min using PBS and blocked against non-specific binding of secondary antibodies for 1 h by means of the blocking medium, containing 5% foetal bovine serum (FBS, Biochrome AG) diluted in 0.1% Triton-X. Cells were rinsed three times with PBS and then reacted with the primary antibodies for 1 h at room temperature. Following this they are again rinsed three times with PBS and incubated with the secondary antibodies (1 h at room temperature). After the immunostaining, all samples were mounted onto microscopy glass slides using a drop of ProLong[®] Gold Antifade (Invitrogen) and were placed at 4 °C until they were investigated using a SP8 CW gated-StED microscope (Leica Microsystems GmbH, Mannheim, Germany) for confocal laser scanning microscopy (cLSM). Samples were examined using 20x/0.75 or 63x/1.40 (both HC PL APO CS2, Leica Microsystems) oil immersion objectives. Furthermore, sample surfaces were investigated using the reflection mode of the microscope to correlate the adhesion sites with the surface nanopattern, induced by the CNT features.

3. Results

3.1. Bulk conductivity of CNT-silicone rubber

Bulk conductivity was determined via 4-point-measurements on already cured samples, as well as on samples cured during application of a dc-field to the material. The already cured samples showed a steep increase in conductivity for low amounts of CNTs using both kinds of CNTs, as Fig. 2 shows. After crossing the percolation threshold, the conductivity rises only slightly. Using Baytubes, the conductivity values for 0.75% (w/w) and 2.5% (w/w) were below 1×10^{-1} S/m. Best results were achieved using 12.5% (w/w) Baytubes leading to a conductivity of 1.2×10 S/m.

Using NC7000, 10-fold higher conductivities could be measured with amounts of CNT below 5% (w/w), starting with values of 3.1×10 S/m at 3.8% (w/w) CNTs. The highest tested amount was 9.6% (w/w) NC7000 leading to an average conductivity of 1.6×10^2 S/m.

Using direct current on a sample without curing agent, it is observed, that CNTs move to the cathode and start forming ramifications from the anode towards the cathode, leading to an almost CNT-less zone at the anode. This has been shown using a compound with a very low amount of CNTs (0.15% (w/w)) in uncured silicone rubber under a light microscope (Fig. 3.). Since this behaviour could be verified, the benefit of alignment was further investigated.

Using higher amounts of CNTs as in Fig. 3 and also adding curing agent, it is not possible to visualize the ramifications. Instead, to evaluate changes in the material during alignment with a specific voltage, the current was monitored. When the resistance heating has cured the silicone rubber, the resistance in the material does not change any further. Fig. 4 shows, that the increase in conductivity due to alignment using high amounts of CNTs is insignificant for samples using NC7000 but show improvement for samples using Baytubes. While improvements for NC7000 stay at about 10%, alignment of the material containing 5% (w/w) Baytubes improves the conductivity by about 95%.

3.2. Etching

Wet etching of the electrode materials surface, that will serve as an interface towards neuronal cells later on, is used to decrease the impedance on the electrode surface by reducing the layer of silicone rubber on the conducting CNTs. Etching the CNT-silicone rubber with TBAF leads to a significant reduction of the insulating layer on the CNTs on sample surface compared to unetched samples.

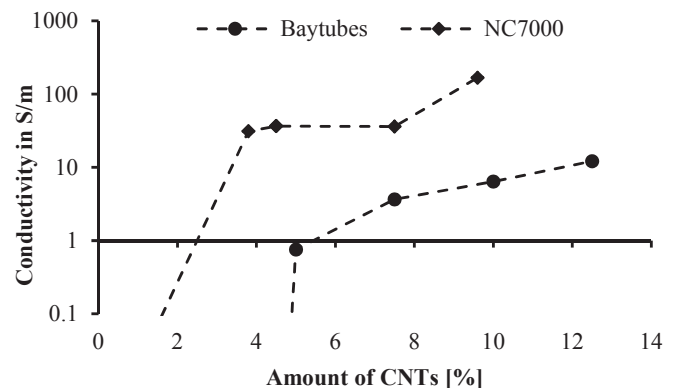


Fig. 2. Medium bulk conductivity of CNT-silicone rubber with Baytubes and NC7000 in varying amounts (according to Table 1).

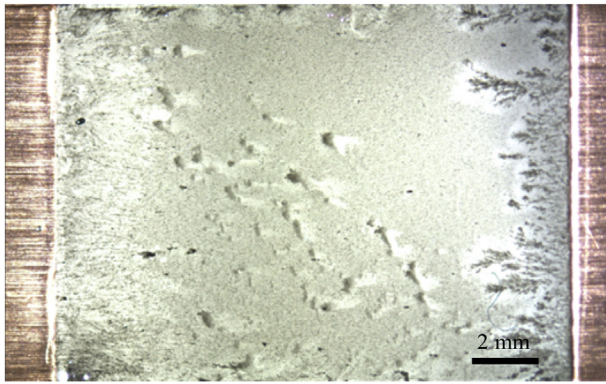


Fig. 3. Alignment of CNTs in CNT-LSR with 0.15% (w/w) CNTs in DC-field at 960 V for 71 min. The compound is between copper pads, with the anode (left) and the cathode (right). CNTs develop ramifications at the cathode while they drift away from the anode.

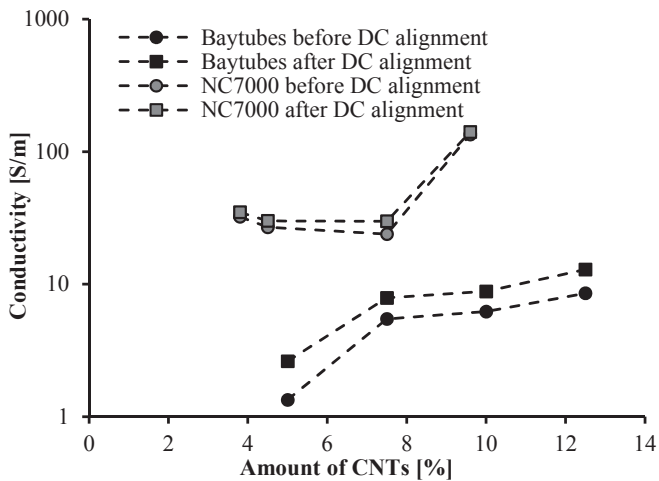


Fig. 4. Medium bulk conductivity of CNT-silicone rubber after alignment in comparison to conductivities before alignment. CNT-amounts used according to Table 1.

As shown in Fig. 5e, the CNTs in the compound are completely immersed in the material and covered with insulating silicone rubber on the interface. Fig. 5 a–d show surfaces which have been etched for 30 min and up to 75 min. An overall improvement regarding the silicone rubber layer on the CNTs is visible in all 4 images, since it is possible to distinguish clusters of CNTs on the sample surfaces. The amount of clusters varies in the samples, which may be rather due to not yet improved mixing techniques, than the etching process. Comparing the brightness of CNTs in the images, etching for 45 min shows the best etching results. They do not visibly improve further after etching for 60 min or 75 min where less CNTs are shown as bright and more seem to be covered in a layer of silicone rubber, suggesting that possibly a first layer of CNT has been completely etched off instead of completely removing residual rubber from the individual CNTs. Using NaOH as an etchant to remove silicone rubber from CNTs, similar results with perfectly visible CNTs, but residual rubber remaining on them can be shown. Fig. 6 shows samples etched for 30 min and up to 75 min with NaOH. The surfaces after 60 min and 75 min etching time are also shown in a close up. Using NaOH it appears, that the results improve with the etching time. The CNTs shown in the images have a medium diameter of 40 nm. With Baytubes mean diameter at approx. 15 nm, this leaves a residual rubber layer of approx. 13 nm on the CNTs. The same surface changes were observed etching silicone rubber compounded with NC7000. With these CNTs, the CNTs in SEM images after etching have a very similar thickness, which leads to a slightly thicker residual rubber layer after etching, since their mean diameter is approx. 9 nm.

3.3. Electrochemical impedance spectroscopy

The impedance measurements were done for the etching times 15 min, 30 min and 60 min on both CNT-silicone rubber materials comparing both etchants. Measured impedances were normalised to be able to compare them to other data. Table 2 shows typical data of specific samples. It can be seen, that the longer surfaces are etched, the lower the measured impedance is. Material surfaces made with Baytubes show a significant difference in the impedance of the surfaces when etched with NaOH or TBAF. While the lowest

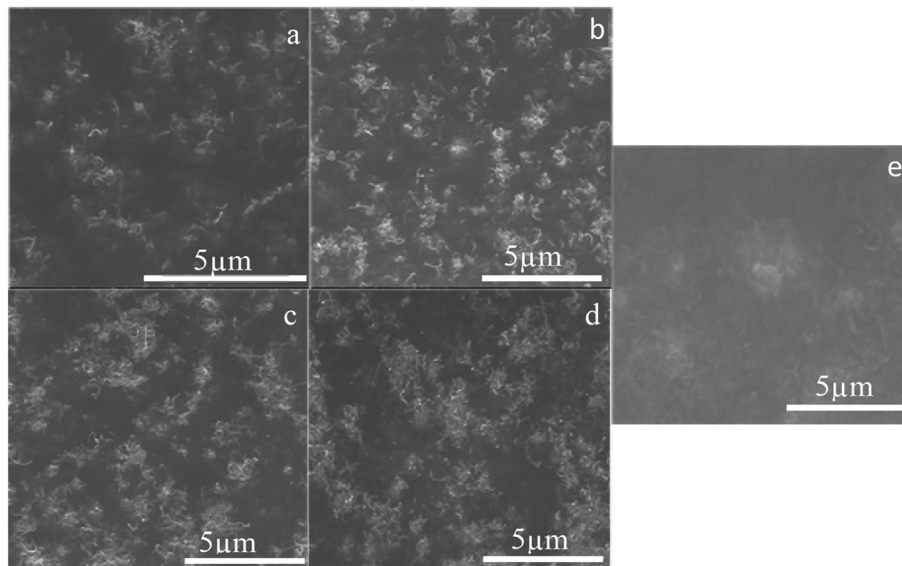


Fig. 5. SEM images of CNT-silicone rubber surfaces with Baytubes, etched with TBAF for a) 30 min, b) 45 min, c) 60 min and d) 75 min and e) unetched surface.

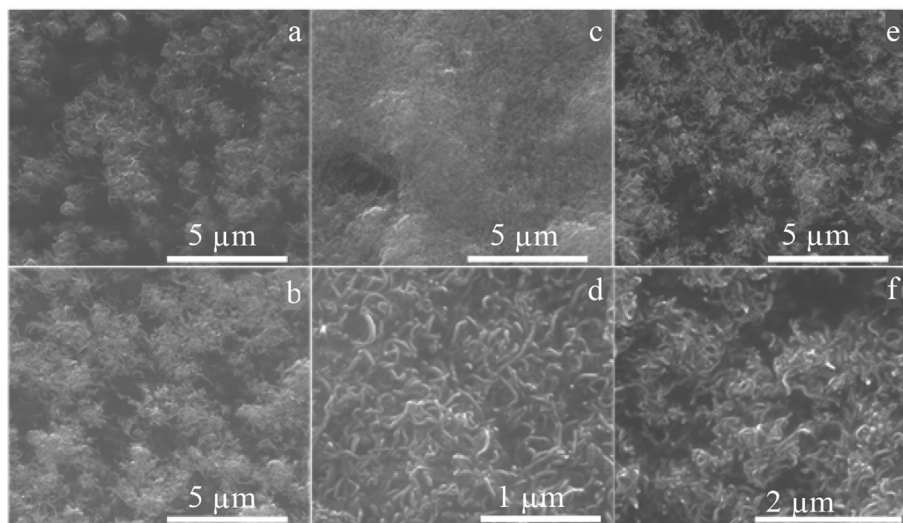


Fig. 6. SEM-Image of CNT-silicone rubber sample with Baytubes wet etched with NaOH for a) 30 min, b) 45 min, c/d) 60 min, e/f) 75 min. Images d and f are enlarged images.

Table 2

Impedances at 1 kHz for selected CNT-silicone rubber samples.

Surface material	Etching duration in min	NaOH impedance in Ωcm^2	TBAF impedance in Ωcm^2
Baytubes	0	4.9×10^{2a}	
	15	5.7×10^2	2.7×10^2
	30	3.5×10^2	1.7×10^2
	60	2.7×10^2	1.3×10^2
	75	2.1×10^2	1.3×10^2
NC7000	0	4.5×10^{2a}	
	15	2.1×10^2	2.7×10^2
	30	1.9×10^2	1.3×10^2
	60	1.5×10^2	1.3×10^2
	75	1.3×10^{2a}	
Gold	0		

^a Impedance of unetched samples in Ωcm^2 .

impedance for NaOH is $2.7 \times 10^2 \Omega\text{cm}^2$, this is the highest impedance in TBAF etched surfaces. This difference does not show in NC7000 compounds where all etched surfaces have significantly lower impedances compared to the unetched surfaces. Besides the CNT-silicone rubber, also a glass substrate sputtered with gold was measured. The results for this sample are with $1.3 \times 10^2 \Omega\text{cm}^2$ identical to the results for both compounds etched with TBAF for 60 min. Using a simple R-R||C model, the CNT-silicone rubber impedance in the capacitive regime was found a factor 1.5 lower compared to the gold substrate. Also the 3 dB roll off frequency was improved to 800 Hz from 1.1 kHz (Gold).

3.4. Biocompatibility tests

Lentivirally GFP-labelled murine fibroblasts were seeded on CNT-silicone rubber surfaces as describes in chapter 2. Fig. 7 illustrates the growth of these fibroblasts after 72 h of cultivation on a silicone rubber control surface and on the CNT-silicone rubber surface variations produced with Baytubes. As it can be observed in these fluorescence microscopic images, fibroblasts developed monolayers on all surfaces and showed normal morphology with over 70% cell growth on all surfaces. A minor decrease in fibroblasts' growth was observed on unetched CNT-silicone rubber surfaces, when compared to the cell growth on silicone controls. Cell growth was slightly increased on both etched CNT-silicone rubber surfaces when compared to unetched CNT-silicone rubber composite surfaces (Fig. 7). The same cell line cultivated on CNT-silicone rubber surfaces produced with NC7000 showed similar results. The cells

also developed monolayers and showed regular cell morphology. Fig. 8 shows the amount of cell growth on each surface in percent. In contrast to the material with Baytubes, here the unetched CNT-silicone rubber shows a somewhat higher percentage of cells growing on it, than on the pure silicone. Interestingly, more cells grow on the surfaces etched with TBAF than on the surfaces etched with NaOH. Still also on all sample surfaces, the cell growth is over 70%.

Since the fibroblasts showed promising cell growth and morphology on the samples, neuroblastoma cells were used, to investigate the behaviour of neuronal cells. Fig. 9 illustrates how neuroblastoma cells adhered onto and grew on silicone rubber control surfaces as well as on all different CNT-silicone rubber surfaces produced with Baytubes for this test. Clearly, the neuron-like cells adhered well onto silicone rubber control surfaces and also onto both etched and unetched CNT-silicone rubber surfaces (Fig. 9). Topographically, two different types of the neuroblastoma cells could be observed. While some cells showed flattened morphology, also known as substrate adherent and therefore called S-Type cells (indicated by F in Fig. 9C), others showed elongated neurite-like extensions and are therefore known as neuroblastic cells or N-type cells (visualized by N in Fig. 9C). More elongated cells were observed on CNT-silicone rubber surfaces etched with TBAF for 60 min, compared with unetched CNT-silicone rubber surfaces or with surfaces etched for 45 min. Moreover, when SH-SY5Y cells were cultured on CNT-silicone rubber surfaces, higher rates of filopodia branching (illustrated by circles in Fig. 10 A, B and D) were observed.

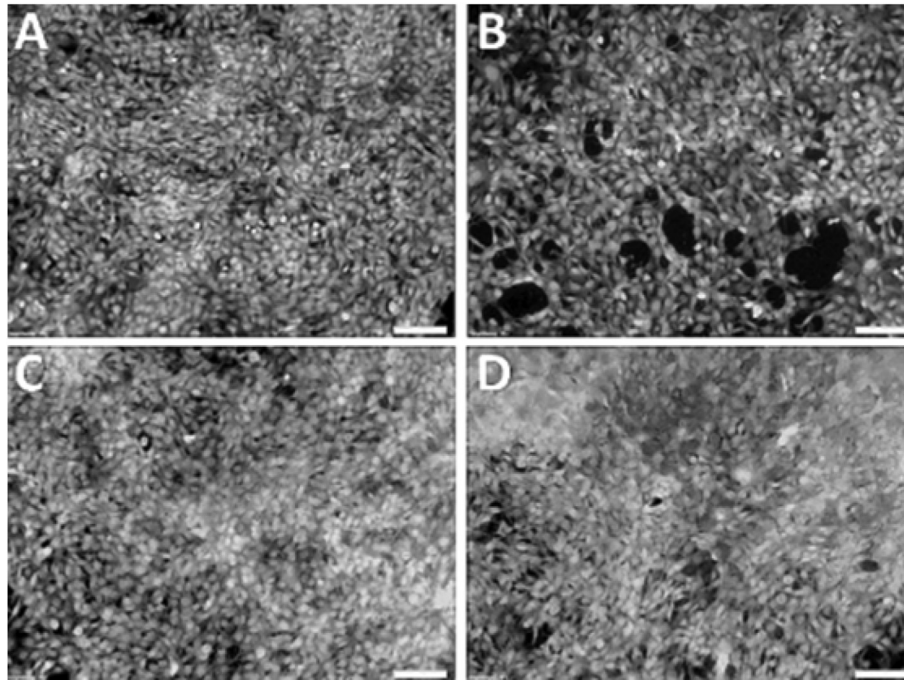


Fig. 7. Fluorescence microscopic images of GFP-labelled NIH3T3 fibroblasts cultivated on different CNT-silicone rubber surfaces produced with Baytubes: A) Sylgard 184, B) CNT-silicone rubber, C) CNT-silicone rubber, TBAF 45 min and D) CNT-silicone rubber, TBAF 60 min. Scale bars indicate 100 μm .

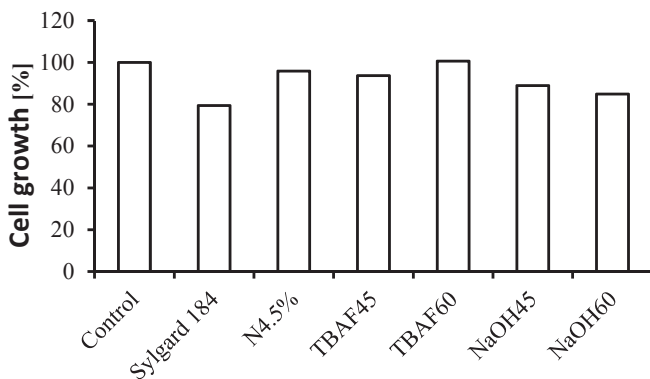


Fig. 8. Cell growth on CNT-silicone rubber surfaces produced with NC7000. Samples were etched with TBAF as well as NaOH for 45 min and 60 min.

To evaluate the cell metabolisms of the material, the WST-1-Assay was established. The amount of reduced tetrazolium to purplish formazan is given as percentage in the diagram in relation to the light intensities detected in control well plates. Fig. 11 shows the percentage of viable cells, when cultivated with different Bay-tube samples, while Fig. 12 shows the results for NC7000 samples. As shown in Fig. 11, added 100% DMSO (positive control) to induce cell death was highly toxic (cell viability < 25%).

All samples including the bare silicone surfaces and CNT-silicone rubber samples showed cell viability of more than 70% indicating non-toxic properties of silicone rubber and all CNTs surfaces according to DIN EN ISO 10993-5. Compared to pure CNT-silicone rubber, the etched surfaces show a better cell viability that increases with the etching duration as shown with the etchant TBAF (Fig. 11 and 12). The results for the surfaces etched with NaOH are, compared to TBAF not as good, with a viability just over 70% compared to almost 100% viability (Fig. 12). After the compatibility of CNT-silicone rubber samples with the neuron-like cells was

revealed, cLSM was used to further investigate topographic characteristics generated by CNT imbedded in silicone, on the adhesion of single SH-SY5Y cells and their processes. Especially the cell adhesion on the surface was investigated. Therefore SH-SY5Y cells were immuno-stained for NCAM to reveal adhesion sites, as well as for NF to observe whole processes.

Figs. 13 and 14 show how single neuroblastoma cells as well as their extensions adhered onto silicone rubber and onto different CNT-silicone rubber surfaces. While most single SH-SY5Y cells adhered well onto silicone surfaces and possessed elongated morphology with straightforward directed extensions (Fig. 13, A–D), extensions of the cells cultured on CNT-silicone rubber surfaces tended to change their direction at certain points. Furthermore, growth cones of cells often were more flattened and showed elevated cell-substrate interaction areas, as well as branching points, when cultivated on CNT-silicone rubber surfaces in comparison to silicone surfaces (Fig. 14). Overlays of reflection mode channel images (left column in Fig. 14) indicate that CNT-caused surface nano-patterns do not have a negative impact on cell adhesion.

4. Discussion

4.1. Bulk conductivity

As shown in chapter 3.1 the conductivity of a CNT-silicone rubber electrode material depends, among others, on the used CNTs. The results show 10-fold higher bulk conductivity in the compound with NC7000 ($3,1 \times 10^1 - 1,6 \times 10^2 \text{ Sm}^{-1}$) than the compound produced with Baytubes ($7,6 \times 10^{-1} - 1,2 \times 10^1 \text{ Sm}^{-1}$). According to a review article by Bauhofer et al. [27] these results are located in the upper spectrum of conductivity in materials using CNT amount between 5 and 10% (w/w) as conductive filler in polymers. For these materials, conductivity lay between $1 \times 10^{-5} - 5 \times 10^2 \text{ Sm}^{-1}$. In contrast to the compound used in this article, most of the CNTs in the mentioned compounds were not

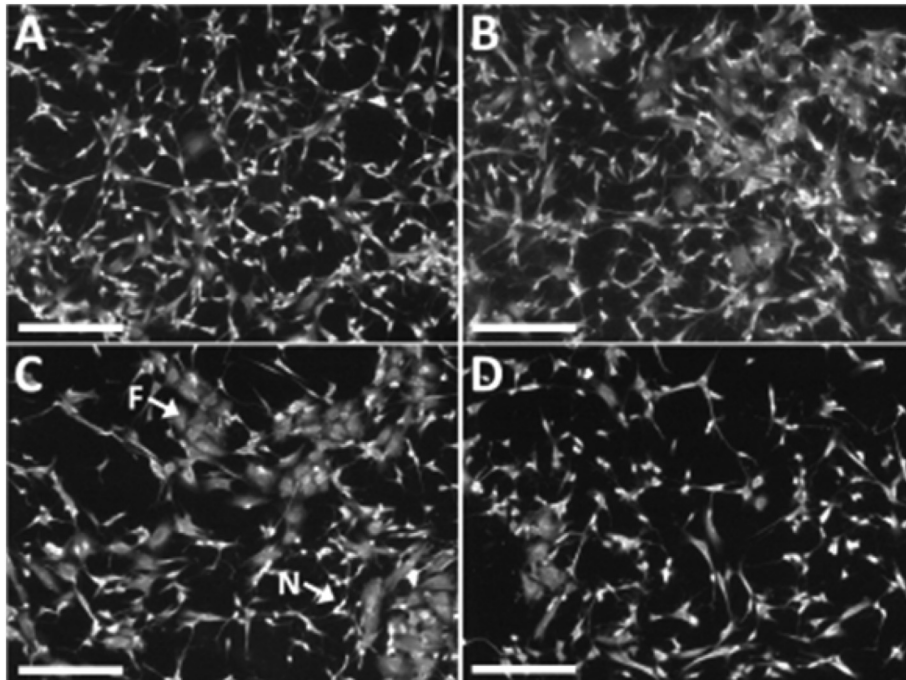


Fig. 9. Fluorescence microscopic images of differentiated human SH-SY5Y neuroblastoma cells on A) pure silicone rubber surface and CNT-silicone rubber with Baytubes B) unetched, C) TBAF-etched for 45 min and D) for 60 min. F indicates flattened and N elongated neuron-like cells in image C. Scale bars mark 200 μm .

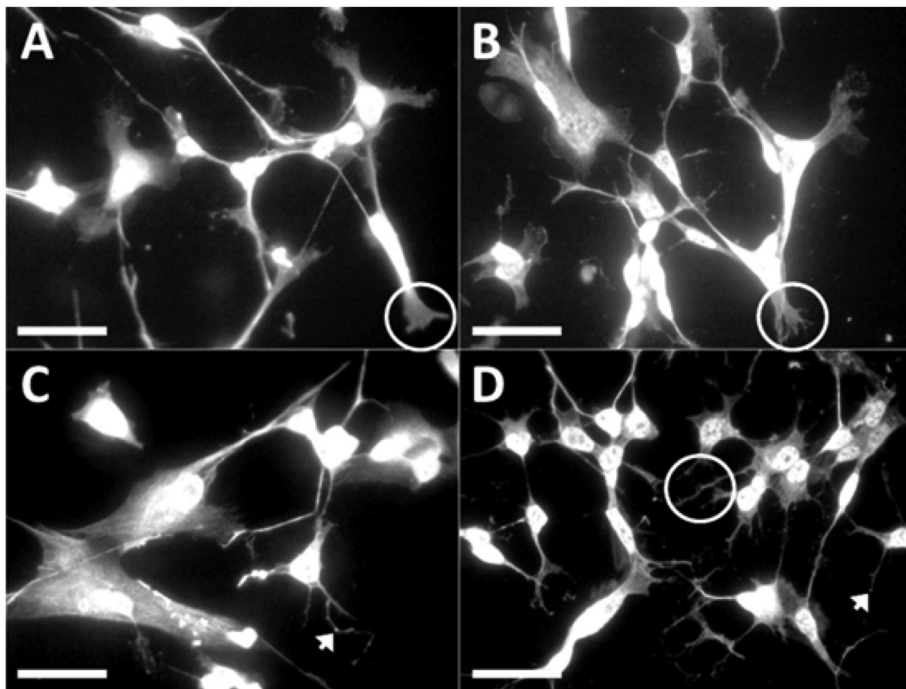


Fig. 10. Fluorescence microscopic images of SH-SY5Y cells on A) silicone control surface and on CNT-silicone rubber with Baytubes B) unetched surface, C) etched with TBAF for 45 min, D) etched with TBAF for 60 min. Filopodia branching is circled in the images. Scale bars measures 30 μm .

mixed by hand, but using one of the common mixing techniques and also functionalized or dispersed in fluids, to obtain improved dispersion. Regarding this, it is expected to gain higher conductivity using an adequate mixing procedure combined with alignment of CNTs. Associated with the difference in the conductivity just mentioned, it is necessary to immerse by far more Baytubes to get

results close to the conductivity of NC7000, which includes much higher viscosity of the CNT compound. Yet, beneficial for the use of Baytubes is, that it is possible to add a higher amount of CNTs to the silicone rubber, before the compound gets to brittle to produce any electrodes. Its brittleness is the reason, why the highest amount of NC7000 was 9.6% (w/w), while with Baytubes also 12.5% (w/w)

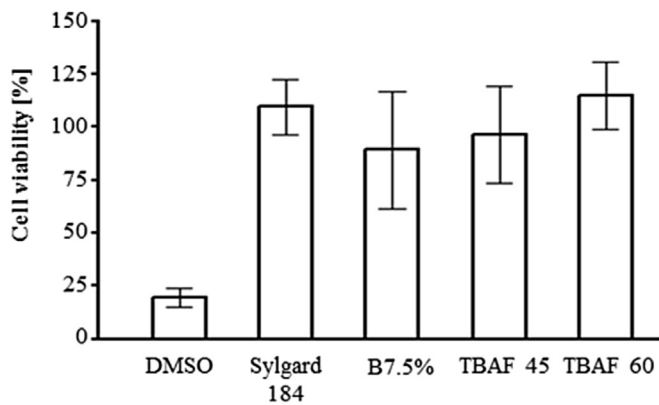


Fig. 11. Results of the WST-1 assay for Baytube samples show cell viability in %, and are presented in Mean \pm SE.

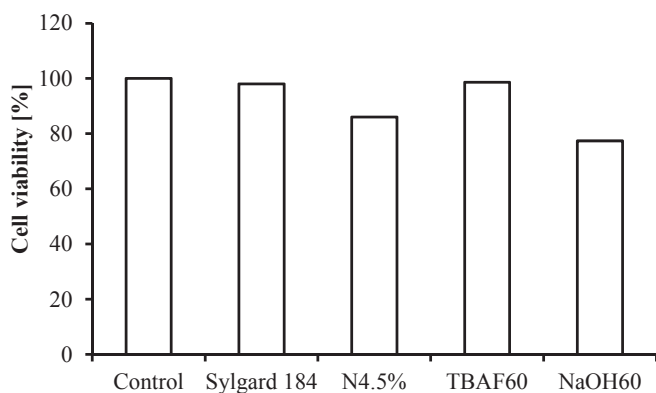


Fig. 12. Results of WST-1 Assay on CNT-silicone rubber produced with 4.5% (w/w) NC7000. Samples are pure Sylgard 184 as well as etched with TBAF and NaOH.

were possible.

DC-alignment of a compound with only 0.15% (w/w) of CNTs and without curing agent was done to investigate the behaviour of CNTs and their polarization in silicone rubber. Martin et al. [28] already showed that CNTs build ramifications from one pole towards the other. This can depend on the properties of the used polymer, wherefore the results for their epoxy resin, could not be directly transferred to silicone rubber. It was shown, that the same kind of ramifications branching happens in silicone rubber, yet the CNTs have a different polarization. While in epoxy, the ramifications start building at the anode, CNTs in silicone rubber are charged positively and start moving towards the cathode where they start branching, leaving less CNTs at the anode. It has been shown for carbon black, that the chemical nature of hardener in an epoxy system is responsible for the charge of filler particles due to different chemical reactions with the surface groups of the filler [29]. This is most certainly also the reason for an opposed polarization of the CNTs.

Since this has been verified for the CNT-silicone rubber and the alignment of CNTs in polymer matrices leads to improved electrical properties in other studies, alignment experiments were done with both compounds and all mentioned weight percentages. Since the electrode material is only of use, when properly cured, the prepolymer compound is already mixed with the curing agent for these tests. Resistance heating lead to a fast curing of the samples, leaving only a small time frame to actually align the CNTs. When cured, the materials conductivity did not change anymore. Still, the difference between both CNT-materials again is significant. In this

experiment, for some of the Baytube materials it was possible to almost double their conductivity, while the changes in NC7000 material stayed below 10% for all amounts of CNT. This may be due to faster curing or, as it can be suspected looking at SEM images of pure NC7000 and by working with this more grainy material, due to a higher rate of entanglement and agglomeration in these CNTs.

4.2. Etching

Etching of the CNT-silicone rubber surfaces, was necessary, to remove the insulating silicone rubber of the CNTs. Nevertheless, a thin layer of silicone rubber is still wanted to ensure the immersion of the CNTs in the bulk material and keep them from leeching from the material and finding their way into the body. This goal was possible to achieve, since the so called residual rubber is not very likely to be removed. As the images in chapter 3.2 show, it is also not very easy to etch as much silicone rubber off to end up with a very thin layer of it on the CNTs. Still, the different etching times are also visible in the images, which show, especially for NaOH etched surfaces, more clearly visible CNTs the longer the etching continues. Also for TBAF it is visible that etching frees the CNTs of silicone rubber. Still in the images of both etchants, the CNTs have diameters around 40 nm leaving them, depending on the kind of CNTs, with at least 13 nm of silicone rubber on them. In congruency with these images, impedance measurements reveal, that longer TBAF etching for 60 min, which does not seem to have an effect compared to 30 min in the images, has an impact on the impedance. For both materials and both etchants, the impedance drops with the etching duration. Compared to the 4-point measurements, the impedance differences for both materials are not very high. This may be caused, by the similar surface topography of the investigated materials. Also possibly the silicone rubber layer on the Baytubes may be thinner compared to the NC7000 material, since the measured diameters are very similar, but the mean diameter of the CNTs are quite different. In comparison to the gold sample, the unetched samples have high impedances, but as soon as they are etched, especially for 60 min, the impedances are converging. The capacitive behaviour of the electrode interface meets the demands of active stimulating electrodes quite well. However, there is still room for improvement towards higher capacitances, as the average PDMS insulation thickness on the CNT may be reduced from 13 nm down to 5 nm, where the onset of charge carrier tunneling may appear.

4.3. Biocompatibility tests

Using cell growth and morphology tests with fibroblast, the biocompatibility of CNT-silicone rubber compound with both kinds of CNTs was established. Fibroblast showed monolayers on all surfaces and also presented good cell morphology on all samples. Cell growth increased on samples with CNTs in comparison the plain silicone rubber samples. It was also revealed, that the etched surfaces were even better suited for the cell growth of fibroblasts. Interestingly samples etched with TBAF showed a better cell growth, than samples etched with NaOH, indicating, that the surface topography and/or chemical properties were more suitable for cell growth. Nevertheless, all samples showed cell growth of well over 70%.

When comparing results for fibroblasts and SH-SY5Y cells a difference in the total amount of cells on the surface can be noticed. These samples show a lot less cells, even though more were seeded into the wells. This can be explained by the retinoic acid, which is used after only 24 h of proliferation time to differentiate the cells into neuroblastoma cells, stopping the cell proliferation. More important than the amount of cells visible is in this case the cell

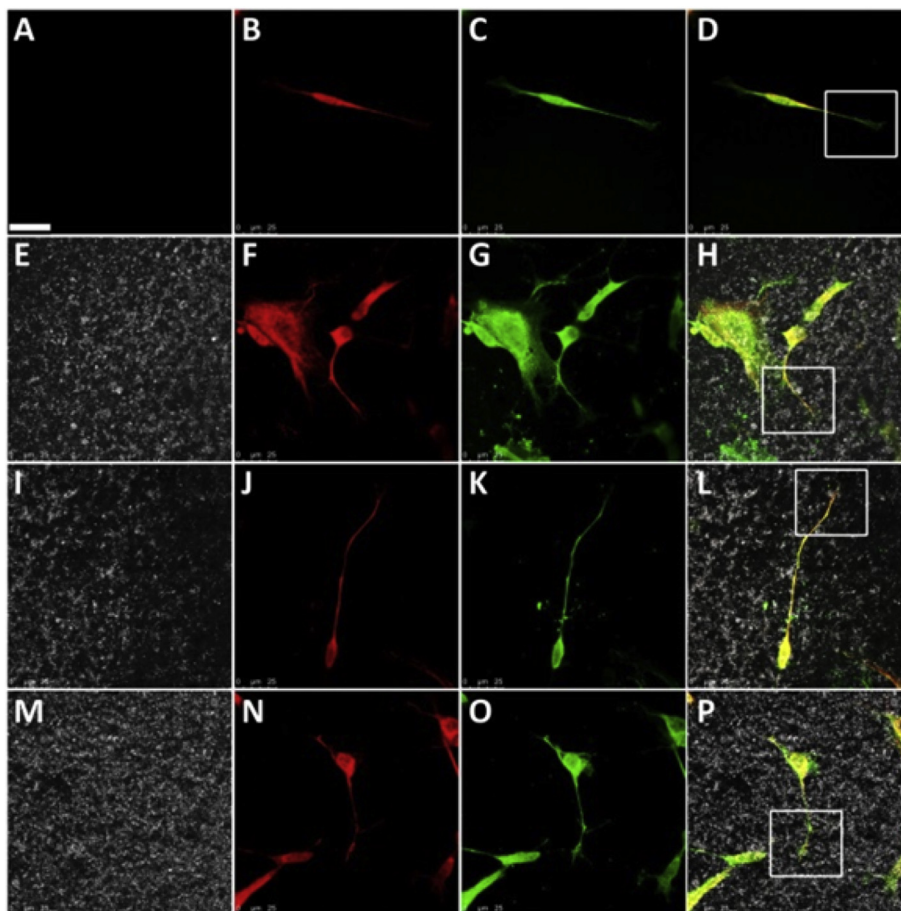


Fig. 13. cLSM images of SH-SY5Y cells grown on silicone rubber control (A, B, C, D), unetched CNT-silicone rubber with Baytubes (E, F, G, H), and TBAF etched CNT-silicone rubber for 45 min (I, J, K, L) and for 60 min (M, N, O, P). The reflection channel is shown in gray scale, NF in red and NCAM in green. Scale bars show 25 μm . (For interpretation of the references to colour in this figure legend, the reader is referred to the web version of this article.)

morphology and development of neurites and branches. Both N-Type and S-Type neuroblastoma cells can be found on the tested samples. As it could be shown, the surfaces all showed a good cell growth and neurite development with partly quite long and branched neurites. Interestingly more SH-SY5Y cells had developed into N-Type cells on the substrate etched longest with TBAF, while many S-Type cells grew on the unetched CNT silicone rubber surface. This may lead to the conclusion, that the surface properties of the etched material trigger the development of N-Type cells far better than the unetched surfaces. Filopodia branching also seems to be triggered more by the etched surfaces, than by the unetched material and silicone rubber. That might be due to the fact, that the uncovered CNTs have diameters, much more similar to neurofilaments, which has already been shown to increase neurite growth on materials [15]. Therefore the etched material seems to be suitable for application in neuronal stimulation.

To evaluate the adhesion of the cells to the material, NCAM were visualized by immuno-cytochemistry. Using cLSM it was revealed, that the cells actually adhere on all tested surfaces and mostly all along the neurofilaments. It was shown, that on silicone rubber, the cells show straight growth, while on CNT-silicone rubber surfaces, the neurofilaments tend to bend at certain points, changing their direction of growth. From the investigation so far it is not possible to find a plausible connection between this behaviour and the CNT-surface. But it can be said, that no behaviour could be seen, where the cells would rather grow on the few silicone rubber surfaces where no CNTs are visible than on the CNTs. In congruency with the

cell growth tests, here also the filopodia branching is more excessive on the CNT surface and it can also be shown, that these filopodia actually all adhere.

The WST-1 assay shows increased cell viability, since the conclusion can be drawn, that a high metabolism indicates good cell viability. The viability even increases with increasing etching duration. In contrast to the cell growth test, in this test the silicone rubber samples showed the highest metabolism rate. Even though, this test shows very good results for all CNT surfaces with viabilities above 70%. The results are in congruency with the cell growth test where lower viability of NIH3T3 fibroblasts was found on the unetched CNT-RTV2 surfaces in comparison to etched surfaces. It was also shown, that TBAF etched samples results in a higher cell viability than samples etched with NaOH.

In terms of biocompatibility, additional testing has to be performed in order to fulfil all requirements of ISO 10993 for medical devices. One might address the encapsulated catalysts (Ni, Co, Fe) that come with industrial grade of MWCNT used in this work. Whilst they can be widely reduced by purification steps, their residues need careful observation. Another important aspect is the mechanical stability of the anchoring of PDMS encapsulated MWCNT-strands. Their possible leaching into body fluids and further transport into sensitive organs needs investigation. Even though the CNT will, due to the bonding strength, remain PDMS covered they are still of nano-size. Whilst they might behave similar to cosmetic PDMS nanoparticles, dedicated investigations have not been performed so far.

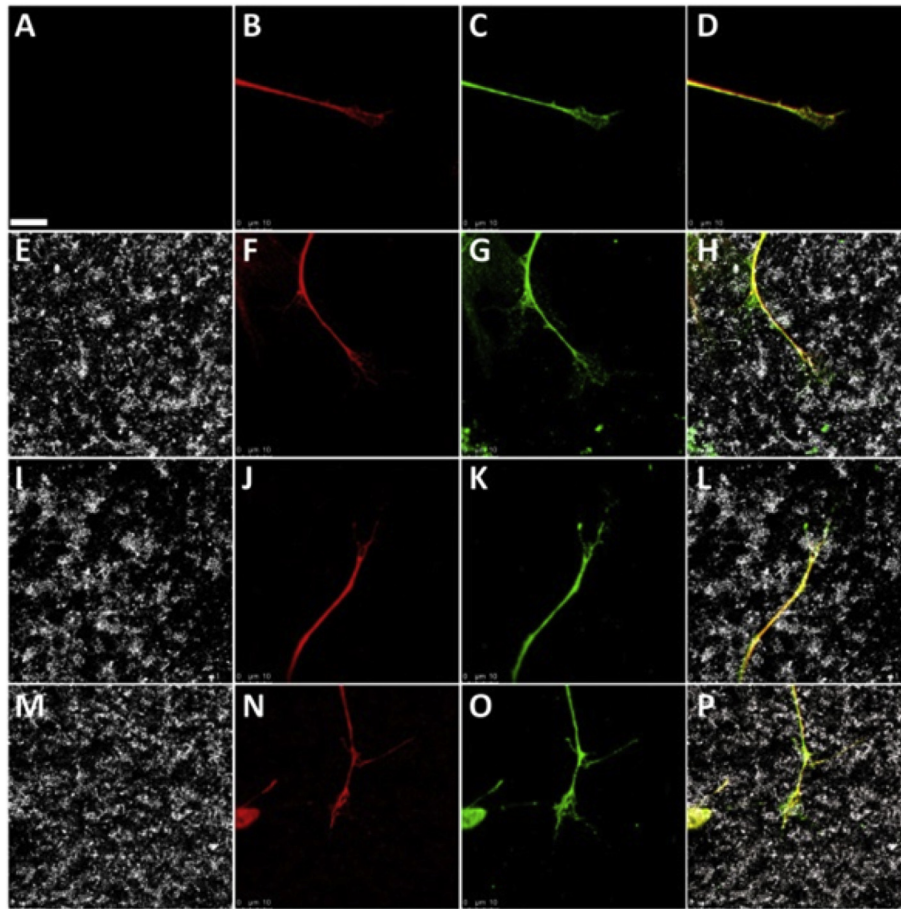


Fig. 14. Higher magnified cLSM images of SH-SY5Y neurites depicted from Fig. 13 (visualized by white squares in Fig. 13). Channel constellations are the same as in Fig. 13 with gray scale for reflection mode, red for NF and green for NCAM. Overlay images are shown in the right column. Scale bars indicate 10 μm . (For interpretation of the references to colour in this figure legend, the reader is referred to the web version of this article.)

5. Conclusion and outlook

Deploying wet etchants, namely TBAF and NaOH, resulted in the desired goal of freestanding CNTs anchored to the PDMS matrix of the CNT-silicone rubber bulk material. The residual rubber was reduced that far, that an estimated layer of only 13 nm is still covering the CNTs and thus securing them to the electrode material. Changes in the surface topography were visualized using SEM and impedance measurements confirmed the etching success. It was revealed that longer etching results in lower impedances, leading to the best result of $1.3 \times 10^2 \Omega\text{cm}^2$ at 1 kHz on a CNT-silicone rubber surface containing NC7000, which was etched with TBAF for 60 min. This is identical to the impedance measured on a gold substrate. In terms of bulk conductivity, measuring CNT-silicone rubber containing NC7000, a conductivity of $1.6 \times 10^2 \text{ S/m}$ was achieved. Cell viability as well as growth and morphology tests show results >70% for all surfaces which even increases on etched surfaces, indicating, that the surface properties are suitable for a biomaterial. Tests with neuroblastoma cells also revealed amplified filopodia growth in comparison to unetched surfaces and silicone rubber. Overall, the bulk conductivity may be further improved, using mixing techniques that will allow a homogenous distribution of CNTs in the PDMS. Also the residual rubber layer may be even further improved using different wet etching techniques or dry etching. In terms of biocompatibility, additional long term and in vivo testing is pending with special attention to leach-resistance of MWCNT-PDMS strands into body fluids.

Acknowledgements

We thank Alexandra Bondarenkova and Oliver Lammers for their help providing data and images of the cell tests and analysis. We thank Janine McCaughey for her help with cell culture and the corresponding cLSM imaging.

This project is supported by the Deutsche Forschungsgemeinschaft, Cluster of Excellence 'Hearing4All' EXC 1077 and German Federal Ministry of Education and Research, KMU-Innovativ: Medizintechnik FKZ 13GW0050B.

References

- [1] D.R. Merrill, M. Bikson, J.G. Jefferys, Electrical stimulation of excitable tissue: design of efficacious and safe protocols, *J. Neurosci. Methods.* 141 (2) (Feb 15 2005) 171–198.
- [2] S.D. Angelov, S. Koenen, J. Jakobi, H.E. Heissler, M. Alam, K. Schwabe, S. Barcikowski, J.K. Krauss, Electrophoretic deposition of ligand-free platinum nanoparticles on neural electrodes affects their impedance in vitro and in vivo with no negative effect on reactive gliosis, *J. Nanobiotechnol.* (Jan 12 2016), <http://dx.doi.org/10.1186/s12951-015-0154-9>.
- [3] S. Yamagiwa, A. Fujishiro, H. Sawahata, R. Numano, M. Ishida, T. Kawano, Chemical Layer-by-layer assembled nanorough iridium-oxide/platinum-black for low-voltage microscale electrode neurostimulation, *Sensors Actuators B* 206 (2015) 205–211.
- [4] K.A. Ludwig, J.D. Uram, J. Yang, D.C. Martin, D.R. Kipke, Chronic neural recordings using silicon microelectrode arrays electrochemically deposited with a poly(3,4-ethylenedioxythiophene) (PEDOT) film, *J. Neural Eng.* 3 (2006) 59–70.
- [5] K. Wang, H.A. Fishman, H. Dai, J.S. Harris, Neural stimulation with a carbon nanotube microelectrode array, *Nano Lett.* 6 (9) (2006) 2043–2048.

- [6] T. Gabay, M. Ben-David, I. Kalifa, R. Sorkin, Z.R. Abrams, E. Ben-Jacob, Y. Hanein, Electro-chemical biological properties of carbon nanotube based multi-electrode arrays, *Nanotech* 18 (2007) 035201 doi:10.1088/0957-4484/18/3/035201.
- [7] A. Mazzatenta, M. Giugliano, S. Campidelli, L. Gambazzi, L. Businaro, H. Markram, M. Prato, L. Ballerini, Interfacing neurons with carbon nanotubes: electrical signal transfer and synaptic stimulation in cultured brain circuits, *J. Neurosci.* (2007) 1051–1107.
- [8] T.C. Liu, M.C. Chuang, C.Y. Chu, W.C. Huang, H.Y. Lai, C.T. Wang, W.L. Chu, S.Y. Chen, Y.Y. Chen, Implantable graphene-based neural electrode interfaces for electrophysiology and neurochemistry in in vivo hyperacute stroke model, *ACS Appl. Mater. Interfaces* 8 (1) (2016 Jan 13) 187–196.
- [9] Cogan FC, Neural stimulation and recording electrodes, *Annu. Rev. Biomed. Eng.* 10 (2008) 275–309.
- [10] P. Fattahi, G. Yang, G. Kim, M.R. Abidian, A review of organic and inorganic biomaterials for neural interfaces, *Adv. Mater.* 26 (12) (Mar 26 2014) 1846–1885.
- [11] S. Iijima, Helical microtubules of graphitic carbon, *Nature* 354 (1991) 56–58.
- [12] H. Cai, X. Cao, Y. Jiang, P. He, Y. Fang, Carbon nanotube-enhanced electrochemical DNA biosensor for DNA hybridization detection, *Anal. Bioanal. Chem.* 375 (2) (Jan 2003) 287–293.
- [13] D.T. Mitchell, S.B. Lee, L. Trofin, et al., Smart nanotubes for bioseparations and biocatalysis, *J. Am. Chem. Soc.* 124 (40) (Oct 9 2002) 11864–11865.
- [14] C. Gaillard, G. Cellot, S. Li, et al., Carbon nanotubes carrying cell-adhesion peptides do not interfere with neuronal functionality, *Adv. Mater.* 21 (2009) 2903–2908.
- [15] G. Cellot, E. Cilia, S. Cipollone, et al., Carbon nanotubes might improve neuronal performance by favouring electrical shortcuts, *Nat. Nanotechnol.* 4 (2) (2009) 126–133.
- [16] S.F. Cogan, Neural stimulation and recording electrodes, *Annu. Rev. Biomed. Eng.* 10 (2008) 275–309.
- [17] N.A. Kotov, J.O. Winter, I.P. Clements, et al., Nanomaterials for neural interfaces, *Adv. Mater.* 21 (2009) 3970–4004.
- [18] H.L. Karlsson, P. Cronholm, J. Gustafsson, L. Moller, Copper oxide nanoparticles are highly toxic: a comparison between metal oxide nanoparticles and carbon nanotubes, *Chem. Res. Toxicol.* 21 (9) (Sep 2008) 1726–1732.
- [19] C. Poland, R. Duffin, I. Kinloch, et al., Carbon nanotubes introduced into the abdominal cavity of mice show asbestos-like pathogenicity in a pilot study, *Nat. Nanotechnol.* 3 (7) (2008) 423–428.
- [20] A. Takagi, A. Hirose, T. Nishimura, et al., Induction of mesothelioma in p53+/- mouse by intraperitoneal application of multi-wall carbon nanotube, *J. Toxicol. Sci.* 33 (1) (Feb 2008) 105–116.
- [21] X. Li, L. Wang, Y. Fan, Q. Feng, F.Z. Cui, Biocompatibility and toxicity of nanoparticles and nanotubes, *J. Nanomater.* (2012). ID 548389.
- [22] A. Beigbeder, M. Linares, M. Devalckenaere, P. Degee, M. Claes, D. Beljonne, R. Lazzaroni, P. Dubois, CH- π interactions as the driving force for silicone-based nanocomposites with exceptional properties, *Adv. Mater.* 20 (2008) 10003–11007.
- [23] M. Perring, M. Mitchell, P.J.A. Kenis, N.B. Bowden, Patterning by etching at the nanoscale (PENs) on Si(111) through the controlled etching of PDMS, *Chem. Mater.* 19 (11) (2007) 2903–2909.
- [24] K. Tegtmeier, P. Aliuos, J. Stieghorst, M. Schickedanz, F. Golly, H. Zernetsch, B. Glasmacher, T. Doll, Aligned carbon nanotube-liquid silicone rubber conductors and electrode surfaces for stimulating medical implants, *Phys. Status Solidi A* 211 (6) (2014) 1439–1447.
- [25] C.A. Schneider, W.S. Rasband, K.W. Eliceiri, [NIH Image to Image]: 25 years of image analysis, *Nat. methods* 9 (7) (2012) 671–675.
- [26] Y.T. Cheung, W.K. Lau, M.S. Yu, et al., Effects of all-trans-retinoic acid on human SH-SY5Y neuroblastoma as in vitro model in neurotoxicity research, *Neurotoxicology* 30 (1) (Jan 2009) 127–135.
- [27] W. Bauhofer, J. Kovacs, A review and analysis of electrical percolation in carbon nanotube polymer composites, *Compos. Sci. Technol.* (2009) 1486–1498.
- [28] C. Martin, J. Sandler, A. Windle, M.K. Schwarz, W. Bauhofer, K. Schulte, M. Shaffer, Electric field-induced aligned multi-wall carbon nanotube networks in epoxy composites, *Polymer* 46 (2005) 877–886.
- [29] M.K. Schwarz, W. Bauhofer, K. Schulte, Alternating electric field induced agglomeration of carbon black filled resins, *Polymer* 43 (10) (2002) 3079–3082.